Journal of
NANOSTRUCTURES
JNS
NANOSTRUCTURES
JNS.kashanu.ac.ir

TEM Characterization and Properties of Cu-1 wt.% TiB_2 Nanocomposite Prepared by Rapid Solidification and Subsequent Heat Treatment

M. Sobhani [*a], H. Arabi [b], A.R. Mirhabibi [c]

[a] *Center of Excellence for high strength alloys technology, School of Metallurgy and Materials Engineering, Iran*
[b] *University of Science and Technology, IUST, Tehran, 16845-118, Iran*
[c] *Center of Excellence for Ceramic Materials in Energy and Environmental Applications, IUST, Tehran, Iran*

Article history:
Received 12/12/2012
Accepted123/2/2013
Published online 1/3/2013

Keywords:
Copper composite
In situ reaction
Nano TiB_2
Solidification
Spinodal

**Corresponding author:*
E-mail address:
m_sobhani@iust.ac.ir
Phone: (+9821) 77459151
Fax: (+9821)77240480

Abstract

Copper matrix composite reinforced by 1wt.% TiB_2 particles was prepared using in situ reaction of Cu-1.4wt.% Ti and Cu-0.7wt.% B by rapid solidification and subsequent heat treatment for 1-20 hrs at 900ºC. High-resolution transmission electron microscopy (HRTEM) characterization showed that primary TiB_2 particles were formed in liquid copper. Heat treatment of as-solidified samples led to the formation of secondary TiB_2 particles via spinodal decomposition of titanium-rich zone inside the grains. Mechanical properties (after 50% reduction in area) as well as electrical conductivity of composite were evaluated after heat treatment and were compared with those of pure copper. The results indicated that, due to the formation of secondary TiB_2 particles in the matrix, electrical conductivity increased along with hardness up to 10 hrs of heat treatment and reached 65% IACS and 155 HV, respectively. Moreover, the maximum ultimate (i.e. 580 MPa) and yield (i.e. 555 MPa) strengths of composite were achieved at this time.

1. Introduction

Copper matrix composite associated with high strength and high electrical conductivity is widely used in industrial applications. Today, different methods have been developed for production of metal matrix composites (MMCs) such as in situ and ex situ methods. In situ reaction has high potential for preparing MMCs with nano-reinforced particles. The fundamental principle of this method is exothermic reaction between elements or between elements and intermetallic compounds within the matrix, which leads to the

formation of in situ ultrafine thermodynamically stable ceramic phases. One of the advantages of in situ reaction is improving interfacial bonding between reinforce phase and matrix because the reinforcement surface remains free of contamination such as gas absorption, oxidation and other detrimental surface reactions [1-3].

Copper matrix composite reinforced by Al_2O_3, TiC, TiB_2 [4-6] and so on has been widely investigated. Among common reinforcing phases, TiB_2 is well-known for enhancing stiffness, hardness, mechanical strength and wear resistance of copper alloys. Furthermore, in contrast to other ceramic reinforcing particles, it has high electrical conductivity. Therefore, the harmful effect of dispersed TiB_2 particles on electrical conductivity of copper is much less than that of other ceramic reinforcing particles [2-3, 7].

Previous studies about strengthening copper matrix by TiB_2 particles via either in situ or ex situ methods have been performed via melt mixing of copper with boron and titanium [2], mechanical alloying [8], stir casting [9] and carbothermic reduction[1]. Manufacturing MMCs composite through rapid solidification and heat treatment process is more of interest due to its lower cost and mass production advantages. Although these processes are commercially available, reports published on the feasibility and characterization of in situ formation of TiB_2 particles through rapid solidification and subsequent heat treatment are limited.

In this research, Cu-1 wt.% TiB_2 composite was fabricated by in situ reaction between boron and titanium in liquid copper. The purpose of this work was to study mechanism of insitu formation of TiB_2 particles in the rapid solidified copper composite as well as mechanical and electrical properties of the produced composite.

2. Experimental procedure

Cu-1.4wt.%Ti and Cu-0.7wt.% B master alloys were prepared from high-purity copper (OFHC), titanium plate (i.e.99.99%) and boron powder (99.98%). These materials were separately melted in an alumina crucible via high vacuum (3.5×10^{-2} mbar) induction melting furnace (VIM) and poured in $50\times50\times100$ mm^3 copper die. The quantitative chemical analysis of the ingots was carried out using inductively coupled plasma optical emission spectrometry (ICP-OES). The quantitative analysis showed composition of Cu-0.69 wt.% B and Cu-1.38wt.% Ti for these ingots and the oxygen content in these ingots was measured as 8.9 ppm and 7.6 ppm, respectively. The ingots were degreased in NaOH solution and cleaned in nitric acid 10%. In order to increase rate of melting and mixing, two master alloys were coupled via simultaneous transferring through an extrusion press. Coupled master alloy was melted in a vacuum induction furnace at 1200°C. In order to avoid gravity segregation, just after melting, the melt mixture was poured in the water-cooled copper die. Heat treatment of cast ingots was performed in the molten salt bath with equal weight percent of NaCl and $CaCO_3$ at 900°C for 1 to 20 hrs. Thin slices were cut from the heat treated samples using ISOMET low speed cutting machine and polished mechanically up to 15µm. 3mm diameter disks were punched out from these samples and then electro-polished via jet electropolisher using solution of 35 % nitric acid and 65% methanol at -30ºC at voltage of 12V. Various samples of as cast and heat treated composite were investigated by high-resolution transmission electron microscopy (HRTEM) equipped with electron energy loss spectroscopy (EELS) and scanning electron microscope (SEM). Hardness tests were performed using Vickers

hardness tester under 30 kgf load. Electrical conductivity in % IACS (International Annealed Copper Standard) of the samples was measured using four-point probe method at room temperature according to ASTM B-193 standard. The heat treated samples were cold worked by rolling up to 50% reduction in the area. The flat type sub-size sample with dimension of 25mm gage length, 6mm width and 1 mm thickness were made from the cold rolled strips. Tensile test with cross head speed of $2mm.min^{-1}$ was conducted at room temperature and the results were compared with those of pure copper. The reported tensile properties were the average of three test results in each condition.

3. Results and discussion

3. 1. Microstructure

Fig.1 shows BS-SEM micrograph of composite. Formation of TiB_2 nano particles (dark region) within the matrix of composite can be clearly seen in this figure. These dark particles were identified as TiB_2 by EDX analysis (Fig1.C). However, as they contain a light boron element, the quantitative analysis by EDX was not precise. Similar observation by TEM and SEM also has confirmed that the in situ chemical reaction between boron and titanium could laed to the formation of TiB_2 particles in molten copper [2-3,6]. As shown in Fig.1.b, the TiB_2 particles that were formed in liquid copper had an irregular shape and almost dispersed in a copper matrix homogeneously. The size of TiB_2 particles is fine but not homogenous. The size of large TiB_2 particles is about 1μm while small size of the particles is less than 100nm. Based on the previous researches, TiB_2 particle size as well as its distribution is affected by many factors including in situ reaction conditions, cooling rate and element concentration [3,10]. Accordingly, in this study, it was thought that the Cu-B and Cu-Ti master alloys cannot be uniformly mixed and completely reacted during melting; hence, the residual titanium and boron solute elements would be absorbed by primary synthesized TiB_2 particles before solidification and result in coarsening and aggregation of smaller TiB_2 particles according to Gou et al. [3]. If both titanium and boron elements can be consumed simultaneously, TiB_2 nano particles cannot be easily coarsened before solidification. Thus, without appropriate solidification rate, aggregation and growth of TiB_2 particles cannot be avoided.

According to solid/liquid interface theories for MMCs [11,12], the distribution of TiB_2 particles (Fig.1.a) are affected by solidification rate . So that, with increasing the solidification rate the distribution of TiB_2 particles were improved and aggregation were reduced. Nevertheless, fine dispersion of in situ formed TiB_2 particles certainly increases the surface energy of the system; therefore, a part of nano TiB_2 particles tends to aggregate in molten copper. Thus, for complete inhibition of aggregation of TiB_2 particles in liquid copper needs precise control of the reaction parameters such as melt mixing condition, reaction time and regular stirring of the melt in addition to solidification rate. This manner was relatively achieved in this study.

Fig. 2 shows HRTEM micrograph of TiB_2 particles within the matrix. This figure demonstrates formation a fair amount of stack fault (Fig2.b) in TiB_2 particles. As the formation of TiB_2 can be considered a diffusion process of boron through titanium melt micelle interface [3], rapid formation and growth of TiB_2 particles in molten copper could lead to an inappropriate arrangement of Ti/B atoms in TiB_2 structure and result in the formation of stack fault. Meng *et al*. [13] reported

a similar mechanism for the formation of stack fault during in situ formation of TiB whiskers.

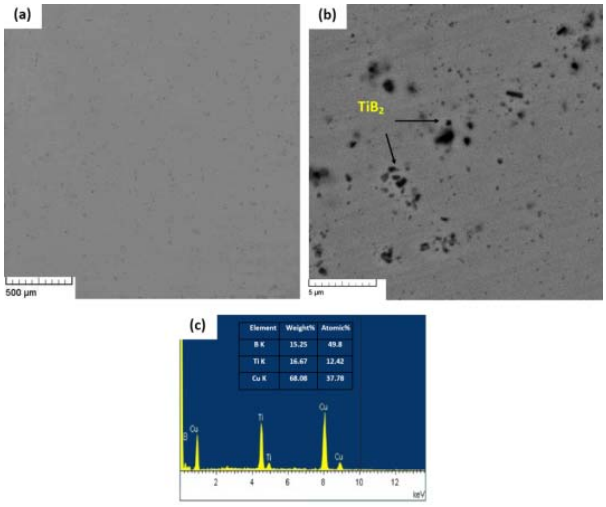

Fig. 1. a) Scanning electron micrograph of TiB_2 particles in copper matrix (b) shape and distribution of TiB_2 particles (c) EDX analysis of TiB_2 particles

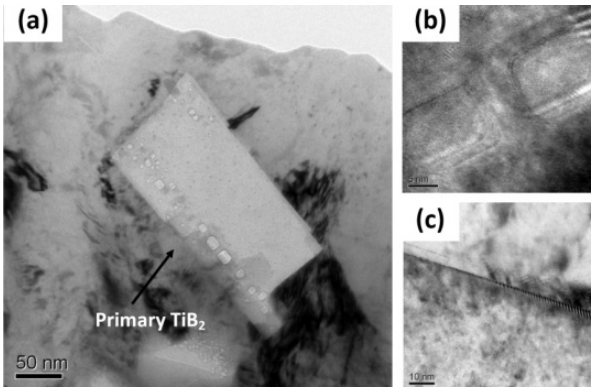

Fig. 2. (a) TEM micrograph of primary TiB_2 particles (b) Stack fault on TiB_2 particles (c) Interfacial bonding between TiB_2 and Matrix

The interfacial surface between copper matrix and TiB_2 particle is shown in Fig2.c. This interface does not exhibit any interfacial byproducts and there is not any transitional layer between them. As can be seen, TiB_2 particles did not react with copper [14] and the interfacial of TiB_2 particulate and copper matrix was clean. Nevertheless, as a result of poor wettability between molten copper and primary TiB_2 particles (i.e. wetting angle=136º [15]), the primary TiB_2 particulate and copper matrix had weak interfacial bonding [16]. The interfacial debonding and/or crack initiation between primary TiB_2 particles and copper matrix can be also seen in Fig.3.c. The reason of interfacial debonding could be analyzed by considering the large difference of elastic modulus and coefficient thermal expansion between copper (16.6×10^{-6} 1/K) and TiB_2 particles (8.2×10^{-6} 1/K), which produces large thermal stress in Cu/TiB_2 interface during solidification. These may lead to interfacial debonding at Cu/TiB_2 interface, which is in agreement with the reported results by Xu et al. [16].

Effect of heat treatment on microstructure of composite was evaluated by TEM. Fig.3.a shows TEM image of composite with jump ratio map of elements via EELS after 6 hrs of heat treatment at 900 ºC. The distribution of elements within the matrix indicates that rapid solidification can suppress chemical reaction between boron and titanium atoms and consequently formation of TiB_2 particles in molten copper. Thus, a part of boron and titanium can freely remain within the matrix after solidification. During heat treatment at high temperature, boron and titanium atoms can react with each other. The result of this reaction is formation of Ti/B compound in the spinodal decomposition region (Fig.3.a). Corresponding to TEM image with the selected area diffraction (SAD) pattern (Fig3.c) and chemical analysis results, it was identified that Ti/B compound is consistent with stoichiometry composition of TiB_2 particles. This figure also confirms that the secondary TiB_2 particles was formed due to spinodal decomposition. The spinodal decomposition has been also reported for

formation mechanism of Cu_4Ti precipitates during age hardening of Cu-Ti alloys [17]. The jump ratio map of elements in spinodal decomposition region revealed that boron segregation was near but not exactly aligned with titanium in self-similar coarsening region (sponge-like structure); however, titanium segregation was seen exactly in alignment with boron in domain fragmentation region. This point indicated that titanium concentration was in form of Cu/Ti alloy rather than Ti/B compounds near high concentration copper areas. HRTEM image along with fast Fourier transformation (FFT) pattern of this region is demonstrated in Fig.3.b. From this micrograph, it can be also observed that the region which was rich in copper and titanium atoms was consistent with stoichiometry composition of Cu_4Ti which had an orthorhombic crystal structure with lattice parameters of a=0. 453 nm, b=0.432 nm and c= 0.1293 nm. This showed that Cu_4Ti can be converted into TiB_2 particles, as confirmed by SAD pattern in Fig.3.c. Thus, it can be concluded that secondary TiB_2 particles might be formed by the following reaction.

$$Cu_4Ti+2B \leftrightarrow TiB_2+4Cu \quad \text{Eq. (1)}$$

Cu_4Ti was replaced with TiB_2 during subsequent heat treatment due to more thermodynamic stability of TiB_2 in comparison to Cu_4Ti [16]. The secondary TiB_2 particles formed based on Eq. (1) were more susceptible in solid state condition according to Dong et al. [8]. They clarified that the activation energy required for the formation of TiB_2 particles on the basis of Eq. (1) was less than that of TiB_2 particles formed directly from boron and titanium atoms.

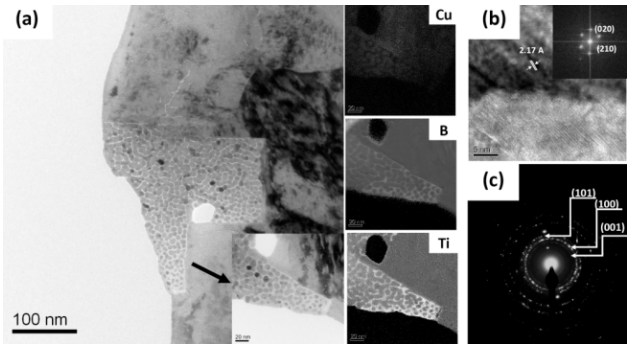

Fig.3. (a) Spinodal decomposition of the secondary TiB_2 particle after 6hrs heat-treatment with jump ratio elements map (b)HRTEM image at copper-titanium interface with FFT pattern of Cu_4Ti (c) SAD pattern of TiB_2 particle

Evolution of spinodal decomposition on formation of secondary TiB_2 during heat treatment is shown in Fig.4. The secondary TiB_2 particles indicated irregular shape as well as primary TiB_2 particles. As shown in this figure, formation mechanism of secondary TiB_2 particles was the consequence of existence of a) spinodal decomposition (shown by arrow "S") and b) refining copper zone (shown by arrow "R").

As the TiB_2 is a stable phase in Cu-Ti-B system, TiB_2 phase is likely to be generated from Eq.(1) and copper intermediate products are remained in TiB_2 particle. With increasing heat treatment time, the fragmented copper was diffused through the TiB_2 structure and finally dissolved in the matrix. Moreover, inter-diffusion among spinodal reaction interfaces led to coarsening TiB_2 particles by the particles' "cannibalizing" each other during heat treatment. This is shown by arrow D in Fig.4.a.

Spinodal decomposition for the formation of secondary TiB_2 particles was especially seen in the confined areas. Nevertheless, development of spinodal decomposition might also occur all over the matrix, as shown by arrow A. Chemical analysis of these regions (Fi.4.c) explained that these areas were rich in Ti as well as B, without

the trace of Cu. This finding explained that it was possible to produce the nano structured copper matrix by accurate control of heat treatment as well as melting condition.

Examination of secondary TiB_2 particulate/Cu matrix interface is illustrated in Fig.4.b., which displays the diffusion interface between TiB_2 particle and matrix. Interfacial stress was not seen between copper/TiB_2 interface. With these pieces of evidence, it can be concluded that interfacial bonding of secondary TiB_2 particles/matrix is better than that of primary TiB_2 particles.

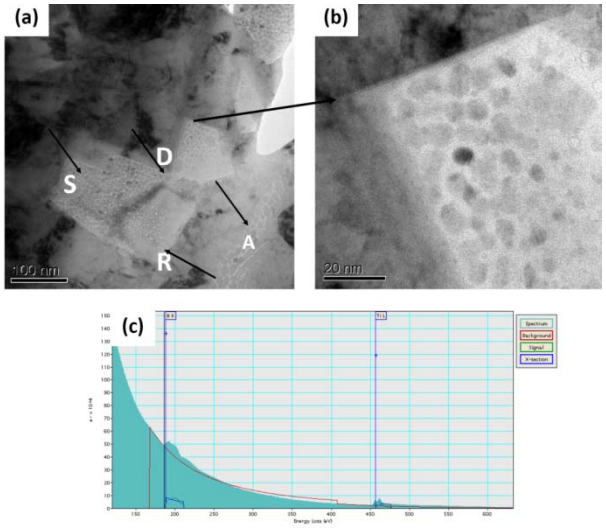

Fig.4. (a) Evolution of spinodal decomposition in composite after 8 hrs heat-treated at 900 ºC, S: Spinodal decomposition zone R: Refined Zone D: Diffusion bonding interface (b)TiB_2/Cu interface, (c) energy-loss spectrum of TiB_2 particles

3. 2. Properties

Effect of heat treatment time on hardness and electrical properties of as rapid solidified samples is shown in Fig. 5(a and b). The hardness of composite gradually increased as time of heat treatment increased. The maximum hardness of composite (155HV) was achieved after 10 hrs heat treatment. The increase in hardness value apparently between 0-10 hrs was most likely due to formation of secondary TiB_2 particles. Based on this result, it could be reasoned that reinforced particles can act as a barrier to movement of dislocation in composite. Thus, more reinforcement particles in the matrix might bring grater increase in hardness correspondingly. After 10 h decrease of hardness happened and effects of secondary TiB_2 formation were completely revoked. Nevertheless, decrease of hardness after the peak value was not remarkable and attributed to the pining effects of TiB_2 particles at grain boundaries, which hindered grain growth at high temperature [7].

Fig. 5b shows variation of electrical conductivity of composite versus heat treatment time. The as cast composite showed electrical conductivity of 50% IACS. Maximum electrical conductivity of composite occurred at 10 hrs; then, it was saturated to a value approximately by 66 % IACS after 20 hrs of heat treatment. As titanium significantly reduced electrical conductivity of copper [18], formation of secondary TiB_2 particles consumed residual titanium in the matrix and electrical conductivity considerably increased. It can be further seen in Fig.5.a,b that increase in electrical resistivity, due to increasing volume fraction of TiB_2 particles, was lower than the decrease in resistivity due to removal of titanium from matrix, which thereby resulted in overall increase in electrical conductivity. This increase in electrical conductivity was mainly due to reduction of scattering surface of conductive electron according to Nordheim rule [19]. The increasing electrical conductivity along with hardness during high temperature heat treatment exhibited that rapid solidified Cu-TiB_2 composite could be used in electrical applications such as high temperature electrical switches and spot welding electrodes and

similar applications required higher strength and lower electrical resistivity.

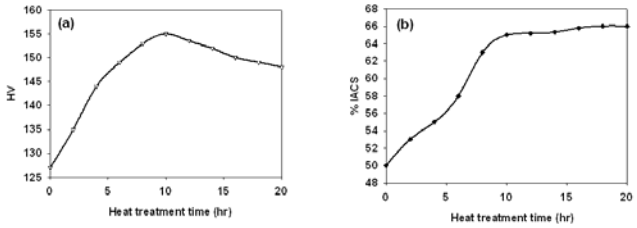

Fig. 5. Effects of heat treatment on (a) hardness and (b) electrical conductivity of composite

Effects of formation of primary and secondary TiB_2 particles on mechanical properties of composite were evaluated and compared with those of pure copper, as listed in Table 1.

Table 1. Comparison of mechanical properties of composite and pure copper

Materials	UTS (MPa)	Ys (0.2 % offset) (MPa)	Elongation %
Composite (5hrs 900ºC)	543	503	13
Composite (10hrs-900ºC)	580	555	10
Pure copper (10hrs-900ºC)	353	280	28

It can be seen that the presence of TiB_2 particles significantly increased yield as well as tensile strength of composite in comparison to those of pure copper. The increasing in mechanical properties is analyzed by considering the interaction between dislocation and TiB_2 particles within the matrix, and in this regard, two strengthening mechanisms could be considered for analysis reinforcement of TiB_2 particles, which are Orowan-loops and Pile-up dislocation mechanisms. The Orowan mechanism suggests that the presence of non-shearable TiB_2 particles (particle size <1μm) within the matrix causes dislocation loop to be left behind after a dislocation line has passed through TiB_2 particles. It also hinders and/or slows down dislocation motion in copper matrix. In addition, for coarse particles (particle size >1μm), the strengthening mechanism is dislocation pile-up between two obstacle particles on slip plane, which leads to increment in yield strength according to Jongsang *et al*. [20].

Formation of secondary TiB_2 particles led to increase in yield strength of composite from 503 MPa to 555 MPa after heat treatment from 5 hrs to 10 hrs and ductility reduced from 13% to 10%. Hence, it seems that secondary TiB_2 particles had not significant effects on ductility of composite and might be attributed to formation of secondary TiB_2 inside the grain rather than grain boundaries and also strong interface bonding between secondary TiB_2 particles and matrix, as shown in Fig.4.b. However, the presence of TiB_2 particles reduced ductility of composite (EL = 10%) as compared to pure copper (EL = 28%), which was due to preferred crack initiation in tensile specimen at these particles according to Tu et al. [1].

4. Conclusion

1-Copper matrix composite reinforced by TiB_2 nano particles was prepared by in situ reaction and rapid solidification. The primary TiB_2 particles were formed in liquid copper. Subsequent heat treatment led to the formation of secondary TiB_2 via spinodal decomposition, which was resulted from the reaction between Cu_4Ti and B. 2- TiB_2 reinforced particles significantly improved hardness and mechanical properties of composite relative to pure copper so that ultimate tensile strength increased by 64% to 580 MPa and hardness increased by about 240% to 155 HV in comparison to pure copper. 3-Electrical

conductivity increased along with hardness and reached 65% IACS after 10 hrs of heat treatment at 900 ºC.

Acknowledgment

The authors would like to express their gratitude to the Iranian nanotechnology initiative for financially supporting this project.

References

[1] J. P. Tu, N.Y. Wang, Y.Z. Yang, W.X. Qi, F. Liu, X.B. Zhang , Mater lett. 52 (2002) 448-452.

[2] J.H. Kim, J.H. Yun, Y.H. Park, K.M. Cho, I.D. Choi, I.M. Park. Mater Sci Eng A. 449 (2007) 1018-1021.

[3] M.X. Guo, K. Shen, M. Wang , Acta Mater. 57 (2009) 4568-4579.

[4] F. Shehata, A. Fathy, M. Abdelhameed, S.F. Moustafa, Mater Des. 30 (2009) 2756-2762.

[5] S. Rathod, O.P. Modi, B.K. Prasad, A. Chrysanthou , D. Vallauri , V.P. Deshmukh, A.K. Shah. Mater Sci Eng. A. 502 (2009),91-98.

[6] M.X. Guo, M.P. Wang, K. Shen, L.F. Cao, Z. Li, Z. J. Zhang. J. Alloys Compd. 460 (2008) 585-589.

[7] Z.Y. Ma, S.C. Tjong, Mater Sci Eng A. 284 (2000) 70-76.

[8] S.J. Dong, Y. Zhou, Y.W. Shi, B.H. Chang. Metall Mater Trans A. 33 (2002) 1275-1280.

[9] T.K. Jung, S.C. Lim, H.C. Kwon, M.S. Kim. Mater Sci Forum. 449 (2004) 297-300.

[10] D. Boˇzi´c, J. Staˇsi´c, J. Ruˇzi´c, M. Vilotijevi´c, V. Rajkovi´c., Mater. Sci. Eng. A. 528 (2011) 8139-8144.

[11] D. Shangguan, S. Ahuja, D.M. Stefanescu. Metall Trans A. 23 (1992) 669-680.

[12] D.M. Stefanescu, B.K. Dhindaw, S.A. Kacar, A. Moitra. Metall Trans A. 19 (1988) 2847-2855.

[13] Q. Meng, H. Feng, G. Chen, R. Yu, D. Jia, Y.J. Zhou. Cryst. Growth. 311(2009)1612-1615.

[14] M. Aizenshtein, N. Frage, N. Froumin, E. Shapiro-Tsoref, M.P. Dariel. J Mater Sci. 41 (2006).185-5189.

[15] G.A. Yasinskaya.Powder Metall Met Ceram. 5 (1966) 557-559.

[16] Q. Xu, X. Zhang, H. X. Han, V.L. Kvani. Mater lett. 57 (2003) 4439-4444.

[17] A. Datta, W.A. Soffa. Acta Metall. 24(1976)987-1001.

[18] S. Nagarjuna, K. Balasubramanian, D.S. Sarma.Mater, Sci. Eng. A. 225 (1999)118-124.

[19] R.E .Hummel, Electronic properties of materials, 3rd. Springer , New York, 2000

[20] L. Jongsang , J. Y. Jung , E.S. Lee, N.J. Kim, S. Ahn. Met Mater Int. 4 (1998) 610-615.